Sensitivity and Power Budget of a Homodyne Coherent DP-QPSK System With Optical Amplification and Electronic Compensation

C. Crognale, *Fellow, IEEE, Senior Member, OSA*

***Abstract*—We numerically and analytically calculate sensitivity and link power budget of an optically amplified electronically compensated dual polarization quadrature phase-shift keying (DP-QPSK) coherent homodyne optical system, taking into account the main parameters of both the optical amplifier and the coherent receiver. After deriving an expression for the signal-to-noise ratio (SNR) of the amplified coherent receiver, we calculate an analytical expression for the optimum local oscillator (LO) optical power which maximizes the SNR, and an approximated closed-form solution for the receiver sensitivity, valid in most of practical cases. This analytical calculation allows to derive, when the impairments of the fiber are compensated, the position of the amplifier into the link that maximizes the optical link power budget. The approximated closed-form solutions are compared with results obtained with a numerical approach. From our investigation it emerges that, in a single-channel fully compensated DP-QPSK coherent system, the performances of both booster and in-line configurations can be even better than that ones of the preamplifier, but they are strongly dependent on the unamplified receiver features, and can require a proper adjustment of the LO optical power, to make the sensitivity compliant with the requirements. Diversely, the performances of a preamplified coherent receiver can be worse, but the amplifier position makes the coherent receiver practically independent on its intrinsic noise sources.**

***Index Terms*—Coherent communications, dual polarization phase shift keying (QPSK), fiber optics links and subsystems, optical communications.**

I. INTRODUCTION

IT is widely held that the coherent optical detection can be considered as the most promising technique today, especially when used together with polarization multiplexing, and advanced modulation schemes [1], [2]. In optical coherent systems, the receiver computes decision variables based on the recovery of the full electric field, which contains both amplitude and phase information [3]. By properly exploiting the features of modern digital signal processing (DSP) techniques, this enables the compensation of linear transmission impairments due to the optical fiber [such as, for example, polarization mode dispersion (PMD), polarization dependent loss (PDL), and chromatic dispersion (CD)], when downconverted signals are sampled at the Nyquist rate [3]. These remarkable features of the coherent optical detection are well-suitable for being merged with those deriving from the use of the optical amplification [1]–[3]: for example, the transmission of Terabit Nyquist wavelength division multiplexing superchannels [1], [2] over thousands of kilometers length fiber links is made possible by properly inserting several optical amplifiers into the link, generally Erbium-doped fiber amplifiers (EDFAs) [4], to interconnect passive fiber spans.

As well-known, in very long-haul coherent transmission systems, the nonlinear impairments introduced by the fiber—i.e., the generation of nonlinear phase noise and nonlinear interference due to the Kerr effect in the fiber [3], [5]—can become particularly severe. Obtaining the best performances of these systems can often require a proper transmission link design, which often consists of adopting a proper management of the launch optical power, capable to assure the maximum signal-to-noise ratio (SNR) at the receiver [5]. On the other hand, in spite of the intrinsic complexity of the algorithms to implement, the effectiveness of modern DSP techniques is increasing more and more day by day, and the electronic compensation is revealing to be even capable to compensate or strongly mitigate the nonlinear impairments due to the optical fiber even in case of very long links, equipped with cascades of tens of amplifiers (e.g., as reported in [6]). Maybe the electronic compensation strategy will not be able to completely solve the problem of the management of nonlinearities in fiber. Nevertheless, the continuous progresses reported in this field lead to foresee that the electronic compensation techniques will allow the full recovery of the detected optical signal in a wide range of cases of practical interest, where the signal degradation introduced by the fiber nonlinearities is significant, but not extreme. Such a situation could be that one of a local area network, for instance, where the transmission of a single-channel coherent polarization multiplexed high-level modulation format signal is made through a quite limited length of fiber, and a single optical amplifier is enough to compensate the power loss due to the fiber attenuation. In this case, it is reasonable to expect that the electronic compensation works well, i.e., it is capable to fully compensate the nonlinearities, or in any case assure a power penalty always below a required maximum value (according to the design specifications), even if the optical signal power is quite high, at the fiber input, or at the output of the amplifier into the link. If we assume that both linear and nonlinear fiber impairments can be compensated only by means of a proper DSP, optimizing the performances of the amplified coherent system in this case means to maximize the optical link power budget with respect to both the optical amplifier key-parameters (given by the peak optical gain value, and the dependence of the optical

Manuscript received September 21, 2013; revised December 15, 2013; accepted December 30, 2013. Date of publication January 1, 2014; date of current version February 19, 2014.

The author is with the Intecs S.p.A., SS.17 Località Boschetto, 67100, L'Aquila, Italy (e-mail: claudio.crognale@intecs.it).

Digital Object Identifier 10.1109/JLT.2013.2297628

gain on the optical input power, in a single-channel transmission), and the coherent receiver characteristics (e.g., LO power, skew-mismatch, thermal noise, and so on).

Just in this context, a recent theoretical work [7] has shown that, when the fiber impairments can be neglected or compensated, the amplifier optical gain saturation features make the allowable optical link power budget of a single-channel amplified digital coherent system strongly dependent on the amplifier position into the link. Moreover, this paper theoretically shows that, when the optical amplifier is used according to a proper in-line configuration, the link power budget of an amplified coherent homodyne BPSK system can increase by tens of dB, with respect to a scheme with the same coherent receiver without amplification. Diversely, as what regards the coherent receiver, an attractive work [8] has recently derived how, in the case of an unamplified application, there is an optimum value of the LO optical power which maximizes the SNR. So, it appears intriguing to investigate the chance of optimizing the performances of a single-channel digital coherent system simply by properly exploiting both the mechanisms of the coherent detection and the optical amplification.

In this paper, we consider a single-channel optically amplified digital coherent homodyne dual polarization quadrature phase-shift keying (DP-QPSK) system, where the fiber impairments are fully compensated (or neglected in any case), and focus our analysis on the performances of the system with respect to the position of the amplifier through the link [7]. First, we derive the SNR of the amplified coherent receiver, taking into account the main parameters of both the amplifier and the receiver: optical gain saturation, ASE, skew mismatch, local oscillator relative intensity noise (LO-RIN), LO optical power, and thermal noise. Then we analytically calculate an expression for the optimum LO optical power which maximizes the receiver SNR. After doing this, we derive an approximated closed-form solution for the amplified receiver sensitivity, i.e., the minimum value of the optical signal power at the optical amplifier input, which is capable to assure a given SNR at the receiver. This analytical calculation, valid in most of practical cases, allows to easily derive the position of the amplifier into the link which maximizes the optical link power budget, when the impact of the fiber linear and nonlinear mechanisms on the signal can be neglected or compensated. In the end, we investigate the performances of the amplified system, by moving the amplifier with respect to the receiver front end. To do this, we numerically find, in correspondence of different amplifiers configurations, the amplified receiver sensitivity, and the corresponding link power budget. Finally, we compare the numerical results with those ones obtained by means of the approximated closed-form approach. Because we assume that the system performances are not affected by the fiber mechanisms, we can consider the results obtained here as the ultimate performances of an optically amplified digital coherent homodyne DP-QPSK system.

II. SNR of the Amplified DP-QPSK Receiver

Let us consider a digital coherent homodyne DP-QPSK receiver, placed at the end of an amplified optical link (according to schematic in Fig. 1) [3], [8]. In presence of a significant NLI, the received complex field vector has been recently expressed [5] as the superposition of the optical signal vector, the ASE field vector, and a perturbative term which takes into account the impact of the NLI mechanism on the receiver SNR. As shown in [5], this approach (based on the assumption—valid after few fiber spans—that ASE and NLI can be considered as additive complex-Gaussian noises) leads to an SNR expression where the total noise variance is made of a sum of noise variances, one of them consists of the LNI noise power, obtained by applying a first-order regular perturbation. As mentioned in the previous section, in our analysis we consider a different scenario, and assume that the DSP algorithm implemented at the receiver side is suitable for fully compensating or strongly mitigating the nonlinear channel impairments, in such a way that the LNI contribution to the SNR can be neglected.

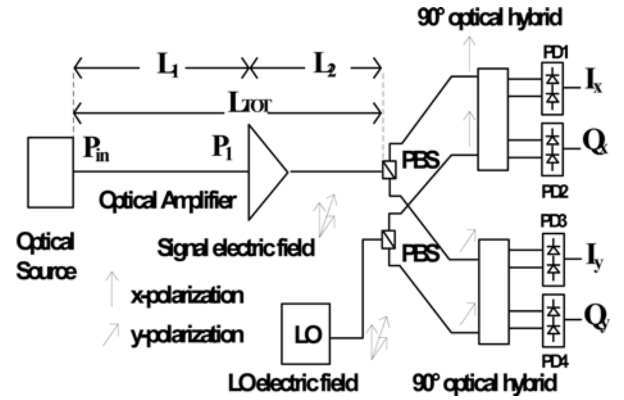

Fig. 1. Schematic of the amplified optical link and the DP-QPSK homodyne receiver.

With this assumption, the total electric field at the receiver input is made of the superposition of the optical signal electric field, the LO electric field, and the ASE electric field [3], [9], [10]. In the transmitter, two synchronous data are phase-modulated in orthogonal polarizations, i.e., x and y. Without any loss of generality, we can refer to the x- and y- polarizations with respect to the principal axes of the polarization beam splitters (PBSs) placed at the input of 90° optical hybrids [3], [9], [10]. After transmission through the fiber, the signal electric field polarization is usually not preserved. For an arbitrary orientated PBS placed at the input of 90° optical hybrids, the received signal can exhibit significant crosstalk between the original signals in the two orthogonal polarization states [10]. For our analysis, we write the optical signal electric field orthogonal components at the PBS into the receiver as [3], [9]:

$$\vec{E}_S = \hat{x}E_{\mathrm{Sx}} + \hat{y}E_{\mathrm{Sy}} \tag{1a}$$

where

$$E_{\mathrm{Sx}} = \sqrt{\frac{\alpha_{11}L_1P_{\mathrm{in}}GL_2}{2}}\exp\left[i\omega_o t + i\varphi_{\mathrm{Sx}}\left(t\right)\right] + \sqrt{\frac{\alpha_{12}L_1P_{\mathrm{in}}GL_2}{2}}\exp\left[i\omega_o t + i\varphi_{\mathrm{Sy}}\left(t\right)\right] + c.c \tag{1b}$$

$$E_{\rm Sy} = \sqrt{\frac{\alpha_{22} L_1 P_{\rm in} G L_2}{2}} \exp\left[i\omega_o t + i\varphi_{\rm Sy}(t)\right] + \sqrt{\frac{\alpha_{21} L_1 P_{\rm in} G L_2}{2}} \exp\left[i\omega_o t + i\varphi_{\rm Sx}(t)\right] + c.c. \quad (1c)$$

In (1b), (1c), $P_{\rm in}$ is the power at the optical link input, L_1 is the link loss at the amplifier input, L_2 the link loss at the amplifier output ($L_{\rm TOT} = L_1 L_2$ is the total link loss), G the amplifier optical gain, ω_o the angular frequency, $\varphi_{\rm Si}$ *(i = x, y)* the phase (containing modulation and noise) of the i-th signal field orthogonal polarization component. α_{ij} (*i,j* = 1,2) parameters introduced in (1b), (1c) take into account the impact of the optical signal field polarization drifting (much slower than the transmission data rate) in a simple way. Terms containing α_{12} and α_{21} represent the crosstalk contributions. As reported in [10], the polarization changes due to the fiber are usually described by a unitary Jones matrix J, and are typically managed by means a proper optical dynamic polarization control technique at the receiver, or with a proper DSP, capable to estimate the terms of the Jones matrix. Because, in our investigation, we consider all channel impairments introduced by the fiber (PMD, PDL, CD, polarization crosstalk) neglected or compensated, we assume, in (1b), (1c), $\alpha_{11} = \alpha_{22} = \alpha = 0.5$, and $\alpha_{12} = \alpha_{21} = 0$. With the same formalism, the LO electric field at the receiver input is:

$$\vec{E}_{\rm LO} = \hat{x} E_{{\rm LO}x} + \hat{y} E_{{\rm LO}y} \quad (2a)$$

$$E_{{\rm LO}x} = \frac{1}{\sqrt{2}} \sqrt{\frac{P_{\rm LO} + \delta P_{\rm LO}(t)}{2}} \times \exp[i\omega_o t + i\varphi_{{\rm LO}x}(t)] + c.c. \quad (2b)$$

$$E_{{\rm LO}y} = \frac{1}{\sqrt{2}} \sqrt{\frac{P_{\rm LO} + \delta P_{\rm LO}(t)}{2}} \times \exp[i\omega_o t + i\varphi_{{\rm LO}y}(t)] + c.c. \quad (2c)$$

with $P_{\rm LO}$, $\delta P_{\rm LO}(t)$, and $\varphi_{{\rm LO}i}$ $(i = x, y)$ which respectively indicate the LO optical power, the LO intensity noise, and the phase noise of the i-th LO field orthogonal polarization component [4], [11]. The ASE field in the optical bandwidth $B_{\rm opt}$ can be represented as a sum of terms with a random phase φ_{ki} $(i = x, y)$ [12]:

$$\vec{E}_{\rm ASE} = \hat{x} E_{{\rm ASE}x} + \hat{y} E_{{\rm ASE}y} \quad (3a)$$

$$E_{{\rm ASE}x} = \sum_{k=-B_\upsilon}^{k=B_\upsilon} \sqrt{2N_O \delta\upsilon} \cdot \exp[i(\omega_o t + 2\pi k \delta\upsilon) + i\varphi_{kx}] + c.c. \quad (3b)$$

$$E_{{\rm ASE}y} = \sum_{k=-B_\upsilon}^{k=B_\upsilon} \sqrt{2N_O \delta\upsilon} \times \exp[i(\omega_o t + 2\pi k \delta\upsilon) + i\varphi_{ky}] + c.c. \quad (3c)$$

in which $B_\upsilon = B_{\rm opt}/(2\delta\upsilon)$, and $N_o = n_{\rm SP}(G\text{-}1)L_2 h\upsilon$ ($n_{\rm SP} = 1.6$ is the amplifier spontaneous emission factor, $h\upsilon$ is the photon energy, $B_{\rm opt}$ the optical bandwidth). With these assumptions, a straightforward calculation leads to the expression (4) shown at the bottom of the page, for the SNR at each couple of balanced photodiodes (*PDj*, $j = 1, \ldots, 4$) of the amplified receiver (neglecting any mixing among noises and signal terms), where

$$I_{\rm Sig}^2 = \alpha R^2 P_1 G L_2 P_{LO} \varepsilon_{12}^2 k(\tau) \quad (5)$$

$$\sigma_{\rm Shot}^2 = 2qRB_N \alpha \varepsilon_{12} P_1 G L_2 + 2qRB_N \varepsilon_{12} \frac{P_{\rm LO}}{2} + 2qRB_N \varepsilon_{12} n_{\rm SP} h\nu (G_o - 1) L_2 B_{\rm opt} \quad (6)$$

$$\sigma_{\rm Sig-ASE}^2 = 2R^2 \alpha P_1 G_o L_2 \varepsilon_{12}^2 {\rm CMRR}_{-} n_{\rm SP} h\nu \times (G_o - 1) L_2 B_N \quad (7)$$

$$\sigma_{\rm P_{LO}-ASE}^2 = 2R^2 P_{\rm LO} \varepsilon_{12}^2 {\rm CMRR}_{+} n_{\rm SP} h\nu (G_o - 1) L_2 B_N \quad (8)$$

$$\sigma_{\rm ASE-ASE}^2 = R^2 \varepsilon_{12}^2 N_o^2 {\rm CMRR}_{\rm ASE} {\rm ASEASE}_{B_N} 2B_N \quad (9)$$

$$\sigma_{\rm RIN-LO}^2 = \frac{1}{4} R^2 P_{\rm LO}^2 \varepsilon_{12}^2 {\rm CMRR}_{\rm RIN} {\rm RIN}_{B_N} 2B_N \quad (10)$$

$$\sigma_T^2 = I_T^2 B_N. \quad (11)$$

In the expressions above, $I_{\rm Sig}^2$ is the average beat signal power detected by each couple of photodiodes in the balanced receivers, $\sigma_{\rm Shot}^2$ the total shot-noise variance (i.e., comprising signal, LO, and ASE contributions), $\sigma_{\rm Sig-ASE}^2$, $\sigma_{\rm PLO-ASE}^2$, and $\sigma_{\rm ASE-ASE}^2$ the signal-ASE, the LO-ASE and the ASE-ASE beat noise terms [12], respectively, $\sigma_{\rm RIN-LO}^2$ the RIN due to the LO (LO-RIN) [4], [11], and σ_T^2 the thermal noise variance. In (5)–(11), $P_1 = P_{\rm in} L_1$ is the optical power at the amplifier input, B_N the electrical noise bandwidth, I_T the signal-independent circuit noise for each double-balanced photodiode (in pA/$\sqrt{}$Hz), $R = (\eta q)/(h\upsilon)$ the responsivity of the photodiodes ($\eta = 0.75$ is the quantum efficiency), α the power ratio of the two optical signal polarization components (introduced above). As in [7], we have taken into account the dependence of the optical gain on the optical input power P_1 by including, into the SNR expression, the well-known functional dependence: $G = G_o/(1 + P_1/P_{\rm sat})$ [4], [13] (with the peak gain $G_O = 31$ dB, and the saturation power $P_{\rm sat} = -18$ dBm). As shown in Fig. 2, this expression fits the real behavior of the gain of an EDFA (as reported in [13]) with a good approximation. In order to derive the impacts of power imbalances and skew mismatches—due to the path length differences at the two inputs of the balanced photodiodes [8]—on the receiver performances, in (5)–(10) we have defined the following parameters: ε, i.e., the power loss due to the mixer (ε = 1/4, in the following section); ε_r, i.e., the power splitting ratio of either the signal port or the LO port to the four sets of balanced photodiodes (as in [8], we have assumed $\varepsilon_r = 1$, in our analysis); $\varepsilon_{12}^2 = \varepsilon^2(\varepsilon_r + 1)^2$ (defined for commodity of notation); τ, i.e. the skew of the four tributaries.

$${\rm SNR}_j = \frac{I_{\rm Sig}^2}{\left(\sigma_{\rm Shot}^2 + \sigma_{\rm Sig-ASE}^2 + \sigma_{P_{\rm LO}-{\rm ASE}}^2 + \sigma_{\rm ASE-ASE}^2 + \sigma_{\rm RIN-LO}^2 + \sigma_T^2\right)} \quad (4)$$

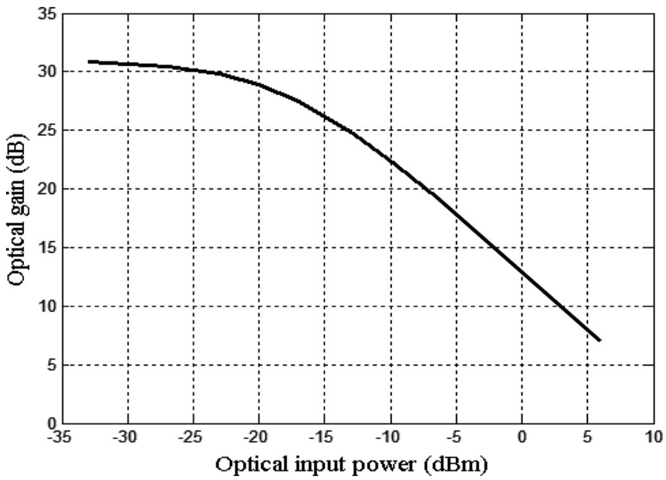

Fig. 2. Amplifier optical gain (dB) versus optical input power (dBm).

Term $k(\tau)$ in (2)–(8) takes into account the impact of the skew τ on the signal. Of course, the influence of the skew on the output signal depends on the particular transfer function of the receiver. Several down-conversion schemes suitable for dual-polarization optical coherent detection are reported in literature (e.g., those shown in [3]), and usually exhibit a great functional complexity. For this reason, an accurate calculation of the skew effects on the detected signal should take into account the particular receiver arrangement, and requires numerical simulations. Diversely, our estimate of these effects is based on an oversimplified model, which however results manageable, and useful in the common practice. So, in the frame of an approximated approach, we do not consider the particular filtering characteristics of the receiver, and model the output of each balanced photodiode as a photocurrent signal given by the subtraction of two currents, each one of them made of a rectangular pulse pattern, with opposite phases with respect of each other, and delayed from each other by τ. In this way, we can easily express the impact of the skew on the signal in term of the reduction of the average output signal power resulting from the unbalancing of the two inputs of the balanced photodiodes. If we assume that, in each time slot T_S, the phase of the i-th signal field orthogonal polarization component takes the values $\varphi_{\mathrm{Si}} = \pi(2n+1)/4$, $n = 0,..,3$ (neglecting noise), the square of the output photocurrent signal level—averaged over the symbol period T_s [14]—can vary within the symbol pattern between a minimum value, equal to

$$I^2_{\min} = \frac{1}{2}2R^2 P_1 G L_2 P_{\mathrm{LO}} \alpha \varepsilon^2_{12} \left[\frac{1}{T_S}\int_0^{T_S-\tau} dt + \frac{(\varepsilon_r-1)^2}{(\varepsilon_r+1)^2}\frac{1}{T_S}\int_{T_S-\tau}^{T_S} dt\right] \tag{12a}$$

and a maximum value, given by

$$I^2_{\max} = \frac{1}{2}2R^2 P_1 G L_2 P_{\mathrm{LO}} \alpha \varepsilon^2_{12} \frac{1}{T_S}\int_0^{T_S} dt \tag{12b}$$

where the $\frac{1}{2}$ factor takes into account the phase modulation contribution. The minimum value in (12a) occurs when, owing to the mutual delay τ between the two inputs, the balanced receiver subtracts—within the time slot T_S—two photocurrent levels which, for a time length $T_S – \tau$ in the time slot T_S, have the same phase (it happens when a mark inversion occurs in the pattern between two subsequent time slots T_S). The maximum value in (12b) occurs when the balanced receiver subtracts two photocurrent levels which, in spite of the skew, exhibit opposite phases, within the time slot T_S (it happens when no signal transition occurs in the pattern between two subsequent time slots). So, in this simplified picture, owing to the skew, the SNR shows pattern dependence, and changes according to the occurrence of these two situations into the output signal pattern. For a QPSK receiver, these two cases occur in both the in-phase and quadrature photocurrent components with the same probability, equal to 0.5, so the average beat signal power of each one of the two orthogonal output signal photocurrent components is given by (5), with a term $k(\tau)$ which can be written as:

$$k(\tau) = \frac{1}{2}\left(\frac{I^2_{\min} + I^2_{\max}}{\alpha R^2 P_1 G L_2 P_{\mathrm{LO}} \varepsilon^2_{12}}\right) = \left[1 - \frac{2\varepsilon_r}{(\varepsilon_r+1)^2}\frac{\tau}{T_S}\right] \tag{13a}$$

with $0 \le \tau \le T_S$. According to its derivation, term $k(\tau)$ in (13a) consists of an average value, which is proportional to the average pulse energy per dibit [3], [14], and is obtained by averaging the signal energy over both the symbol period T_S and the whole pattern. The corresponding expressions in the case of the lowest and the highest values of pulse energy per dibit can be easily derived from (12a) and (12b), respectively:

$$k_{\min}(\tau) = \frac{I^2_{\min}}{\alpha R^2 P_1 G L_2 P_{\mathrm{LO}} \varepsilon^2_{12}} = \left[\frac{T_S-\tau}{T_S} + \frac{(\varepsilon_r-1)^2}{(\varepsilon_r+1)^2}\left(\frac{\tau}{T_S}\right)\right] \tag{13b}$$

$$k_{\max} = \frac{I^2_{\max}}{\alpha R^2 P_1 G L_2 P_{\mathrm{LO}} \varepsilon^2_{12}} = 1 \tag{13c}$$

with $0 \le \tau \le T_S$. For a perfectly balanced receiver, $\tau = 0$, and $k(\tau = 0) = 1$. So, the term $k(\tau)$ in (13a) easily gives the power penalty due to the skew effects on the signal, which adds to that one given by the impact of this parameter on the noise variances. Assuming $\varepsilon_r = 1$ and $\tau = 10$ ps, $k(\tau) = -0.66$ dB, for a DP-QPSK receiver operating at 112.8 Gb/s (i.e., at 28.2 GBaud). If the worst case is considered, i.e., if the lowest value of pulse energy per dibit is taking into account, the power penalty can be expressed by $k_{\min}(\tau)$, which gives the value: $k_{\min}(\tau) = -1.44$ dB, with the same assumptions.

Now let us consider the noise. In (5)–(11), we have defined the following parameters:

$$\mathrm{CMRR}_{\mathrm{RIN}} = \frac{\int_0^\infty |\varepsilon_r - \exp(i2\pi f\tau)|^2 \,\mathrm{RIN}(f)\,|H(f)|^2 df}{(\varepsilon_r+1)^2 \int_0^\infty \mathrm{RIN}(f)\,|H(f)|^2 df} \tag{14a}$$

$$\mathrm{CMRR}_{\mathrm{ASE}} = \frac{\int_0^\infty |\varepsilon_r - \exp(i2\pi f\tau)|^2 \left(1 - \frac{f}{B_{\mathrm{opt}}}\right)|H(f)|^2 df}{(\varepsilon_r+1)^2 \int_0^\infty \left(1 - \frac{f}{B_{\mathrm{opt}}}\right)|H(f)|^2 df} \tag{14b}$$

$$\mathrm{CMRR}_{\pm} = \frac{\int_0^{\infty} |\varepsilon_r \pm \exp(i2\pi f\tau)|^2 \, |H(f)|^2 df}{B_N (\varepsilon_r + 1)^2}. \tag{14c}$$

From a practical point of view, these terms can be considered as generalized expressions of the balanced mixer's effective common mode rejection ratio (CMRR) [8], [15]. According to their definitions, these parameters give the amount of the leakage due to the skew as a function of frequency [15], taking into account the particular spectral shape of the noise power spectral density considered, filtered by the overall receiver transfer function *H(f)* (modeled, as in [8], as a fifth order Butterworth LPF with an electrical noise bandwidth $B_N = 20$ GHz). In particular, the parameter $\mathrm{CMRR}_{\pm}$ refers to noise power spectral densities which can be considered constant within the noise bandwidth B_N: the signal-ASE beat noise, and the LO-ASE beat noise variances, with a negative or a positive sign into the argument of the integral, respectively. We can notice that both $\mathrm{CMRR}_{\mathrm{RIN}}$ and $\mathrm{CMRR}_{\mathrm{ASE}}$ approach the CMRR_{-} expression, in case of constant noise power spectral densities. Then they give an idea of the impact of these noise spectral shapes on the balanced mixer's CMRR. According to this approach, we have also defined the following mean values, averaged on the noise bandwidth B_N:

$$\mathrm{RIN}_{B_N} = \frac{\int_0^{\infty} \mathrm{RIN}(f)\, |H(f)|^2 df}{B_N} \tag{15}$$

$$\mathrm{ASEASE}_{B_N} = \frac{\int_0^{\infty} \left(1 - \frac{f}{B_{\mathrm{opt}}}\right) |H(f)|^2 df}{B_N} \tag{16}$$

where $\mathrm{RIN}_{\mathrm{BN}}$, and $\mathrm{ASEASE}_{\mathrm{BN}}$ refer to the LO-RIN, and the ASE–ASE noise spectral densities, respectively.

III. Optimum LO Optical Power

As shown in (5)–(11), the LO optical power has an impact on both the signal and the overall noise variance of SNR_j in (4). The signal term linearly increases with LO optical power. As what regards the noise, let us first consider the LO-RIN noise variance. The RIN spectral distribution of the LO laser source $\mathrm{RIN}(f)$ in (15)—and then the value of $\mathrm{RIN}_{\mathrm{BN}}$, i.e., the amount of the LO-RIN integrated onto a given noise bandwidth—is defined with respect to the squared mean value of the source optical power, and depends on the laser source bias current [16], [17]. For our analysis, we consider keeping the LO laser biasing current held fixed (i.e., the LO laser source emits a constant CW optical output power), in such a way that the LO-RIN spectral distribution $\mathrm{RIN}(f)$ does not change [4], [11], [16]–[19], and define P_{LO} as the LO optical power detected by each balanced photodetector, which varies independently on the LO laser injection current (for example, by means of a passive optical device inserted in front of the LO laser output). From a practical point of view, this means that we consider $\mathrm{RIN}(f)$ as a constant reference spectral shape, so that—as in [8]—both $\mathrm{CMRR}_{\mathrm{RIN}}$ and $\mathrm{RIN}_{\mathrm{BN}}$ terms in (14a) and (15) can be considered independent on P_{LO}, and the LO-RIN noise variance depends on the detected LO power just as the squared value of P_{LO}. As what regards the other terms in the SNR expression, we can notice from (5)–(11) that both the LO-shot, and LO-ASE beat noise variances increase proportionally with the LO power (as the signal term does), whereas all the other noise variances do not depend on this parameter at all.

As in the case of an unamplified coherent receiver (investigated in [8]), we can expect from this particular functional dependence of SNR_j on P_{LO} that, in correspondence of a given value of the amplifier input power P_1, there is a value P_{LOOPT} of the LO optical power which maximizes the SNR in (4). This can be easily shown by performing the derivative of the SNR in (4) with respect to P_{LO}

$$\begin{aligned} P_{\mathrm{LOOPT}} = \Bigg\{ \Bigg(& \frac{\alpha P_1 G L_2}{\eta \varepsilon_{12}} \\ & + \frac{n_{\mathrm{SP}} h\nu B_{\mathrm{opt}} (G-1) L_2}{\eta \varepsilon_{12}} + \alpha P_1 n_{\mathrm{SP}} G (G-1) L_2^2 \mathrm{CMRR}_{-} \\ & + \frac{n_{\mathrm{SP}}^2 h\nu (G-1)^2 L_2^2 \mathrm{CMRR}_{\mathrm{ASE}} \mathrm{ASEASE}_{B_N}}{2} \\ & + \frac{I_T^2}{2R^2 \varepsilon_{12}^2 h\nu} \Bigg) \cdot \left(\frac{\mathrm{CMRR}_{\mathrm{RIN}} \mathrm{RIN}_{B_N}}{4h\nu} \right)^{-1} \Bigg\}^{\frac{1}{2}}. \end{aligned} \tag{17}$$

As we will show in the following sections, the expression above for the optimum value of P_{LO} allows to numerically derive the best receiver performance.

IV. Sensitivity and Optical Link Power Budget

In order to derive the amplified coherent receiver performances, we will make use of two well-known parameters: the amplified receiver sensitivity and the optical link power budget. By definition, the amplified receiver sensitivity is the minimum value of the optical signal power P_1 at the optical amplifier input which assures a required value SNR_o of $\mathrm{SNR}j$, suitable for obtaining a desired performance of the receiver. The value of SNR_o is usually introduced into the expression of the error probability P_e, and used to derive the bit-error-rate of the receiver (for example, as reported in [3], [9], [14], by means of the complementary error function). By making the $\mathrm{SNR}j$ expression in (4) equal to SNR_o, we obtain an equation which, for a given value of P_{LO}, and in correspondence of a given position of the amplifier into the link, can be numerically solved in term of P_1. The P_1 value derived by numerically solving this equation is the amplified receiver sensitivity P_S. The best amplified receiver sensitivity, i.e., that one obtained in correspondence of the optimum value of P_{LO} compatible with a given configuration of the amplifier, must be calculated by taking into account the dependence of P_{LO} on P_1 (as shown in (17)). This optimum value of the amplified receiver sensitivity can be derived by numerically solving, with respect to the P_1 and P_{LO} variables, a system made of two equations, i.e., that one obtained by making $\mathrm{SNR}j$ in (4) equal to SNR_o, and the other one given by (17).

The value of P_S found by numerically solving the equation for P_1 can be used to derive the optical link power budget of the amplified link. If P_{in} is the optical power at the optical link input, and P_S is the sensitivity of the amplified receiver for a fixed position of the amplifier into the link, the optical link loss compatible with both a required receiver performance and a fixed value of the optical power at the link input is (assuming all fiber impairments compensated or neglected):

$$L_{\mathrm{TOT}} = \left[\frac{P_S\,(L_2)}{P_{\mathrm{in}}} L_2\right]. \tag{18}$$

By definition, this loss is equal to the inverse of the optical link power budget [7]. Then, in this picture, the optical link power budget in unit of dB is simply given by the absolute value of the total link loss L_{TOT}, expressed in the same unit:

$$L(\mathrm{dB}) = -L_{\mathrm{TOT}}(\mathrm{dB}) = -\left[L_2(\mathrm{dB}) + P_S(\mathrm{dBm}) - P_{\mathrm{in}}(\mathrm{dBm})\right]. \tag{19}$$

In the case of the preamplifier configuration, the optical link power budget is given by (19) with $L_2 = 0$ dB, and then it is directly obtained by calculating the difference in unit of dB between the input power P_{in} and the amplified receiver sensitivity P_S. As what regards the booster configuration, we can notice from (19) that the optical link power budget can be derived from the value of L_2 which satisfies the equality: $P_s(\mathrm{L}_2) = P_{\mathrm{in}}$. It is worth noting how the expression of the optical link power budget in (19) increases without any limit, by enhancing the input power P_{in}. This is simply due to the assumption of neglecting all fiber impairments which, in our analysis, are considered compensated or in any case strongly mitigated by a proper DSP. According to this approach, we can consider, as an upper bound of the (19), that one obtained in correspondence of the upper limit value of P_{in} which induces on the signal nonlinear effects too high to be compensated with a DSP technique.

The numerical approach appears the most convenient way to analyze the performances of the link, when all noise sources are taken into account, because it can be implemented without any particular difficulty, and a closed-form solution for P_S in presence of all noise variances results in any case cumbersome and difficult to derive, even for a fixed value of P_{LO}. Diversely, the equation for P_1 becomes manageable when few approximations can be made. In fact, by neglecting the contributions of the signal-ASE, and the ASE–ASE beat noise terms into the SNR expression in (4), we can easily find the following analytical solution for P_S:

$$P_S = \frac{P_{\mathrm{shot}}\left[n_{\mathrm{ASE}}\,(G_o - 1)\,L_2 + K\right]}{\left\{L_2\left[G_o\,(1 - n_{\mathrm{sig-shot}}) + \frac{P_{\mathrm{shot}}}{P_{\mathrm{sat}}}\left(n_{\mathrm{ASE}} - \frac{K}{L_2}\right)\right]\right\}} \tag{20}$$

where, for commodity of notation, we have defined the following parameters:

$$P_{\mathrm{shot}} = \frac{2\,\mathrm{SNR}_o h\nu B_N}{\alpha k(\tau)} \tag{21}$$

$$K = \frac{1}{2\eta\varepsilon_{12}} + \frac{P_{\mathrm{LO}}\mathrm{CMRR}_{\mathrm{RIN}}\mathbf{RIN}_{B_N}}{4h\nu} + \frac{I_T^2}{2R^2\varepsilon_{12}^2 h\nu P_{\mathrm{LO}}} \tag{22}$$

$$n_{\mathrm{sig-shot}} = \frac{P_{\mathrm{shot}}}{2\eta P_{\mathrm{LO}}\varepsilon_{12}} \tag{23}$$

$$n_{\mathrm{ASE}} = n_{\mathrm{SP}}\mathrm{CMRR}_{+} + \frac{n_{SP}h\nu B_{\mathrm{opt}}}{\eta P_{\mathrm{LO}}\varepsilon_{12}}. \tag{24}$$

As we will demonstrate in the next section, the closed-form solution (20) is a valid approximation in most of practical situations, and results very useful to derive the main features of an optically amplified electronically compensated coherent receiver in a simple way. The numerator of P_S in (20) is made of two terms: the first on the left (due to LO-ASE beat noise), depending on the amplifier spontaneous emission factor and the amplifier optical peak gain, and the other one, depending on the characteristics of the unamplified receiver, which are included into the K term in (22). This last parameter linearly increases with the LO-RIN and the thermal noise and approaches the unit value, when both the intrinsic noise variances of the unamplified receiver go to zero. The impact of the first term on P_S decreases as the variable L_2, so that, by moving the amplifier far from the receiver front end, it becomes less and less significant (as L_2 progressively reduces), up to being overcome by the other term due to the unamplified receiver. The denominator of (20) is made of two terms as well: the first one on the left, that consists of the amplifier peak gain (apart from a contribution due to the signal shot noise term $n_{\mathrm{sig-shot}}$, which is usually negligible), and the second one, whose impact decreases with respect to the optical gain saturation power P_{sat}. As we can expect, when the amplifier saturation power decreases, this last term produces an enhancement of the value of P_S (i.e., the required value of optical input power capable to assure a given performance), which corresponds to a reduction of the amplified receiver performances. In the practice, we can consider this term at numerator of (20) as the expression of an *effective* optical gain, whose impact on the denominator decreases (owing to the gain saturation) by progressively reducing L_2 (i.e., increasing the link loss after the amplifier), and produces an increment of P_S. As shown in (20), the *effective* optical gain decrement obtained by enhancing the link loss after the amplifier is as larger as the K term in (22) increases. Because the value of K linearly increases with both LO-RIN and thermal noise, this means that the increment of P_S due to the gain saturation obtained by decreasing L_2 becomes more significant by enhancing the unamplified receiver noise. Finally, we can notice from (20) that, as we can reasonably expect, when P_{sat} is very large and $G_o = 1$, the expression of P_S approaches the sensitivity of the unamplified coherent receiver divided by the link loss after the amplifier: $P_S \sim P_{\mathrm{shot}}K/[L_2(1\text{-}\,n_{\mathrm{sig-shot}})] \sim P_{\mathrm{shot}}K/L_2$. If $L_2 = 1$, and $\tau = 0$, when $G_o \gg 1$ *or* P_{LO} *becomes very large,* P_S *approaches the shot noise limit:* $P_S \sim P_{\mathrm{shot}}/L_2$, with P_{shot} as introduced in (21) [4], [7], [9]. We can insert the approximated solution for P_S given by (20) into (18) to get a useful closed-form expression suitable for deriving the position of the amplifier into the link which maximizes the optical link power budget [7]. In fact, inserting (20) into (18), and by making the first derivative of the resultant expression with respect to the variable L_2, we can find a minimum for the total link loss L_{TOT}. This value of L_2 corresponds to the position of the amplifier into the link which allows to get the minimum value for L_{TOT} according to the input power P_{in}, the amplifier parameters, the receiver characteristics, and the required value SNR_o of the SNR. According to (19), this value also corresponds to the maximum optical link power budget.

A straight forward calculation leads to the following approximated expression for the optimum position of the amplifier:

$$L_{2\mathrm{opt}} = \frac{\left(\frac{P_{\mathrm{shot}} K}{P_{\mathrm{sat}}}\right)\left\{1+\sqrt{1+\frac{P_{\mathrm{sat}} G_o (1-n_{\mathrm{sig-shot}})+P_{\mathrm{shot}} n_{\mathrm{ASE}}}{P_{\mathrm{shot}} n_{\mathrm{ASE}} (G_o-1)}}\right\}}{\left[G_o(1-n_{\mathrm{sig-shot}})+P_{\mathrm{shot}} n_{\mathrm{ASE}} P_{\mathrm{sat}}^{-1}\right]}. \quad (25)$$

It is worth spending few words about this particular feature of the amplified coherent system. In order to explain this result [analytically expressed by means of (25)], firstly let us make some consideration about the main feature of the preamplifier configuration. In this configuration, the performances of the amplified compensated coherent system in essence depend on the characteristics of the optical amplifier (i.e., unsaturated value of the optical gain, LO-ASE beat noise), and the amount of LO optical power. In this case, the sensitivity of the preamplified receiver will be able to approach the shot noise limit [11], leading to an allowable link loss given by [recalling (18)]: $L_{\mathrm{TOT}} = P_S/P_{\mathrm{in}} \sim P_{\mathrm{shot}}/P_{\mathrm{in}}$ (with P_{in} assigned, and $L_2 = 1$). By moving the amplifier far from the receiver, all noise contributions due to ASE will be progressively attenuated by the link loss after the amplifier. Anyway, as long as the LO-ASE beat noise term in the numerator of (20) is dominant, the amplified receiver sensitivity will not vary in a significant way, so that, according to (18), when the amplifier in not very far from the receiver front end, the allowable link loss in unit of dB will decrease almost linearly by reducing L_2. By enhancing the link loss between amplifier and receiver, all noise contributions due to ASE will be strongly attenuated by the link loss after the amplifier. In this way, the amplified receiver sensitivity will approach more and more that one of an unamplified coherent receiver, where the input signal is attenuated by an amount equal to the link loss after the amplifier, and raised up by the *effective* amount of the optical gain compatible with the amplified receiver sensitivity P_S, whose value—given by (20)—must be compliant with the amplifier position L_2. If the amplifier optical gain was independent on the optical power at the amplifier input (i.e., if the impact of the second term depending on P_{sat} in the denominator of (20) was negligible), the sensitivity of the amplified receiver would increases almost linearly by reducing L_2, and—according to (18)—the optical link loss compatible with the link requirements would approach the limit: $L_{\mathrm{TOT}} \sim P_{\mathrm{shot}} K/(G_o P_{\mathrm{in}})$. Then, in this case, the optical link power budget would be the same of that one of the coherent receiver, but enhanced by the gain G_o. With respect to the preamplifier configuration, the optical link power budget would change by an amount on the order of G_o/K. Because this ratio is usually very large, in an amplified coherent receiver, a significant improvement of the optical link power budget would be introduced. On the other hand, owing to the influence of the second term in the numerator of (20) (that takes into account the amplifier gain saturation), this limit value will not be able to be reached: after decreasing up to a value very close to it (obtained in correspondence of a particular position of the amplifier into the link which allows the amplifier to work with a gain $G \sim G_o$), the allowable optical link loss will keeps on increasing (i.e., the link power budget keeps on decreasing), according to the amplifier gain saturation dynamics, up to reaching the maximum saturation point, obtained in correspondence of the booster configuration. In essence, we can consider the optimum amplifier configuration as that one which is obtained in correspondence of a distance of the amplifier from the receiver which allows the amplified coherent system to have the performances of an unamplified coherent system, enhanced by an amount on the order of the unsaturated value of the amplifier optical gain. It is worth emphasizing that, in the approximated expression for the optimum position of the amplifier given by (25), the input power P_{in} does not appear. This means that, in most of practical cases, in a fully compensated link the maximum optical link power budget is obtained in correspondence of a distance of the amplifier from the receiver front end whose value depends on the amplifier and receiver parameters only. In this position of the amplifier, the optical power at the amplifier output is simply: $P_{\mathrm{out}} = P_s \cdot G(P_s)\ L_{2\mathrm{opt}}$, with P_s and $L_{2\mathrm{opt}}$ given by (20), and (25), respectively, and $G(P_s)$ equal to the value of the optical gain for $P_1 = P_s$. This value of optical power can be quite high because, when the amplifier is placed in correspondence of its optimum position, the amplifier optical gain $G(P_s)$ is very close to its peak value. So, we are aware that, in the optimum in-line configuration (and, of course, when the amplifier approaches the booster configuration), the coherent system can strongly experiment the impact of the nonlinear mechanisms induced by the Kerr effect, and the support of an electronic compensation technique could result less effective. According to our assumptions, we do not take into account this problematic, in our theoretical analysis, where we are interested in investigating the ultimate performances of a compensated coherent system, and postpone this topic to a future work. Here we limit ourselves to suggest, as an easy way to overcome the impairments of the Kerr effect in the optimum in-line configuration, the approach of properly reducing the amplifier peak gain, according to the specific compensation capabilities of the DSP algorithm implemented at the receiver side.

V. Theoretical Analysis and Results

We have analyzed a DP-QPSK receiver at 112.8 Gb/s, which detects a wide bandwidth optical ASE noise (i.e., $B_{\mathrm{opt}} = 40$ nm), and is equipped with a LO high-power laser having the LO-RIN spectral distribution RIN*(f)* reported in Fig. 3(a). We have derived this spectral shape from experimental data reported in [16] for a low-RIN high power laser operating at 1550-nm wavelength. The laser frequency response parameters (i.e., resonance frequency, damping factor, and so on [4], [11], [16]–[19]) have been set in such a way to give, in correspondence of a constant CW optical power of 40 mW (i.e., equal to 16 dBm, a typical value of a DP-QPSK coherent receiver), an averaged value $\mathrm{RIN}_{\mathrm{BN}}$ of the LO-RIN equal to -155 dB/Hz. In our analysis, we consider both the spectral distribution $\mathrm{RIN}(f)$ in Fig. 3(a) and this value of $\mathrm{RIN}_{\mathrm{BN}}$ as reference parameters. This value of $\mathrm{RIN}_{\mathrm{BN}}$ is quite realistic, compatible with those usually considered in literature [8], [16], and capable to emphasize the impact of the LO laser noise on the coherent receiver.

Let us analyse the dependence of the SNR on the LO power. For our investigation, we have considered a balanced receiver

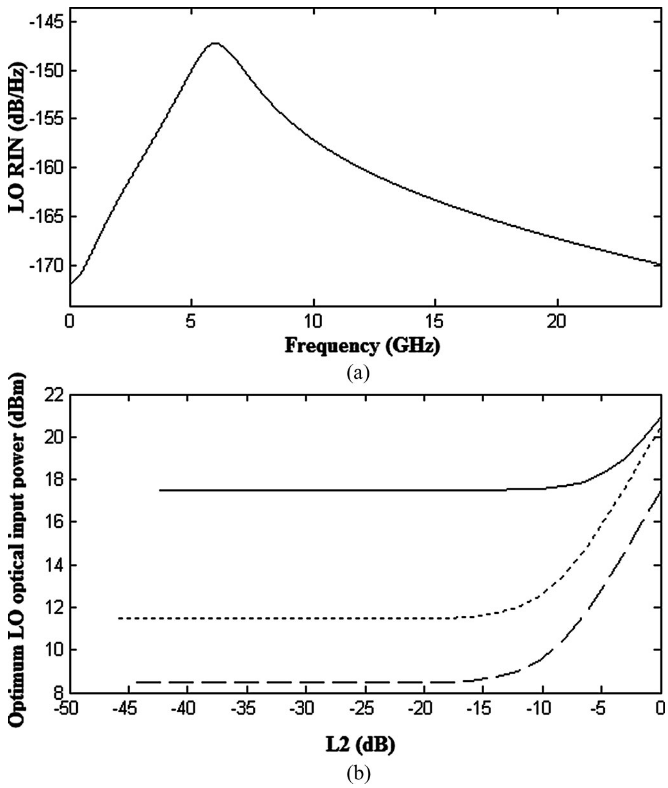

Fig. 3. LO relative intensity noise (dB/Hz) versus frequency (GHz) [see Fig. 3(a)]. Optimum LO optical input power (dBm) versus L_2 (dB) [see Fig. 3(b)] for different values of $\mathrm{RIN_{BN}}$, and I_T ($\tau = 10$ ps).

with 10 ps skew, with the following values of CMRR parameters: $\mathrm{CMRR}_- = -8.80$ dB, $\mathrm{CMRR}_+ = -0.61$ dB, $\mathrm{CMRR_{RIN}} = -12.83$ dB, $\mathrm{CMRR_{ASE}} = -8.80$ dB. Fig. 3(b) reports the optimum LO optical power (dBm) versus L_2 (dB) for three different cases: $\tau = 10$ ps, $\mathrm{RIN_{BN}} = -155$ dB/Hz, $I_T = 18.5$ pA/$\sqrt{\text{Hz}}$ (dotted-curve); $\tau = 10$ ps, $\mathrm{RIN_{BN}} = -149$ dB/Hz, $I_T = 18.5$ pA/$\sqrt{\text{Hz}}$ (dashed-curve); $\tau = 10$ ps, $\mathrm{RIN_{BN}} = -155$ dB/Hz, $I_T = 74$ pA/$\sqrt{\text{Hz}}$ (continuous-curve). In the dashed-curve, the higher value of $\mathrm{RIN_{BN}}$ has been obtained by means of a constant proportionality coefficient, i.e., without changing the LO-RIN spectral shape $\mathrm{RIN}(f)$, and then without modifying the $\mathrm{CMRR_{RIN}}$ parameter. In practice, in this way we have analysed the impact of the LO-RIN on the coherent receiver performances by making a comparison between two similar LO sources, which emit the same optical power at their outputs, but produce, at the inputs of balanced receivers, two LO optical noise variances which differ of 6 dB from each other, in correspondence of the same skew mismatch.

Making a comparison of both the dashed (i.e., the higher LO-RIN case) and the continuous (i.e., the higher thermal noise case) curves with the dotted curve (i.e., the reference curve), we can notice from Fig. 3(b) that, for $L_2 = 0$ dB (i.e., in the preamplifier configuration), the optimum LO power value strongly depends on the amount of the LO-RIN, and is only slightly influenced by thermal noise. The behaviour progressively changes enhancing the optical link loss between the amplifier, and the receiver (i.e., moving the amplifier far from the receiver, towards the booster position): for a link loss higher than $\sim$15 dB, in each curve the optimum LO power level approaches a constant value, and practically becomes the same of that one of the unamplified receiver. According to the figure, in this case, the optimum LO optical power of the amplified coherent receiver is strongly influenced by both LO-RIN and thermal noise. In particular, diversely from the preamplifier, after $\sim$15 dB link loss the impact of the thermal noise on the optimum LO power appears even more significant than that one of LO-RIN. This result is consistent with the functional dependence of P_{LOOPT} as expressed in (17). In fact, we can notice from this expression that the value of the optimum LO optical power increases as the square root of the signal-ASE beat noise, ASE–ASE beat noise, and thermal noise, but decreases as the square root of the LO-RIN. When the amplifier is placed in front of the receiver, the ASE–ASE beat noise is the dominant term in the numerator of (17), because the ASE noise is that one of an unfiltered ASE source, in practice, and the link loss is at the minimum (the contribution of the signal-ASE beat noise is negligible). So, in this configuration, increasing thermal noise only leads to a slight enhancement of the value of P_{LOOPT}, which in essence depends on the ASE–ASE beat noise, and the LO-RIN. According to (17), because P_{LOOPT} decreases as the square root of the LO-RIN, 6 dB of LO-RIN enhancement leads to a decrement of the LO optimum power equal to the square root of the LO-RIN increment itself (i.e., 3 dB).

On the other hand, owing to the functional dependence of P_{LOOPT} on the ASE–ASE beat noise, the optimum LO power value of the receiver decreases by reducing the amount of ASE at the receiver input. This can be done—for example—by introducing an optical filter at the receiver front end or—as considered in Fig. 3(b)—moving the amplifier away from the receiver, in such a way that the ASE power noise exiting from the amplifier results progressively attenuated by the link loss. In this way, the impact of the ASE–ASE beat noise on the numerator of (17) gradually decreases, and the thermal noise becomes more and more significant, up to being the dominant noise term. Over $\sim$15 dB of link loss, up to the booster configuration, the value of P_{LOOPT} mainly depends on LO-RIN and thermal noise, according to the relationship which holds for the unamplified coherent receiver: thermal noise acts in an opposite way with respect to the LO-RIN term, and leads to a strong enhancement of the optimum LO power value, if increased as in the figure, with respect to the reference curve. It is to point out that the LO-ASE beat noise does not appear in (17). In fact, this term acts as a constant noise plateau in the SNR (i.e., just like the shot-noise in an unamplified receiver, as reported in [8]), and does not give any contribution to the value of P_{LOOPT}. Finally, we point out that, in proximity of the preamplifier position (and even for any configuration of the amplifier, in the case of the continuous curve in the figure, i.e., in presence of a very high thermal noise), the optimum LO power P_{LO} overcomes the constant reference value of 16 dBm. In the frame of our theoretical analysis, this means that the LO laser optical power is not high enough to give, in correspondence of both the skew and the particular LO-RIN spectral distribution considered, an optimized performance of the coherent receiver. If the LO laser biasing current can be raised up, the calculation of the optimum LO

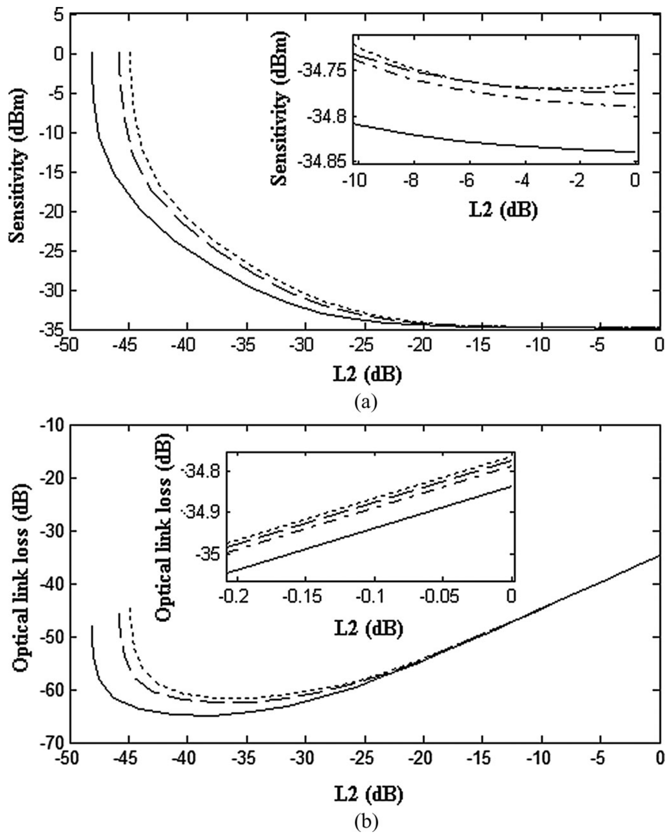

Fig. 4. Sensitivity versus L_2 (dB) [see Fig. 4(a)], and optical link loss (dB) versus L_2 (dB) [see Fig. 4(b)] for different values of τ, and $P_{\rm LO}$ (I_T = 18.5 pA/$\sqrt{}$Hz, $\text{RIN}_{\rm BN} = -155$ dB/Hz, *SNRj* = 13 dB). Dashed, and dashed-dotted curves are distinguishable only in enlarged pictures.

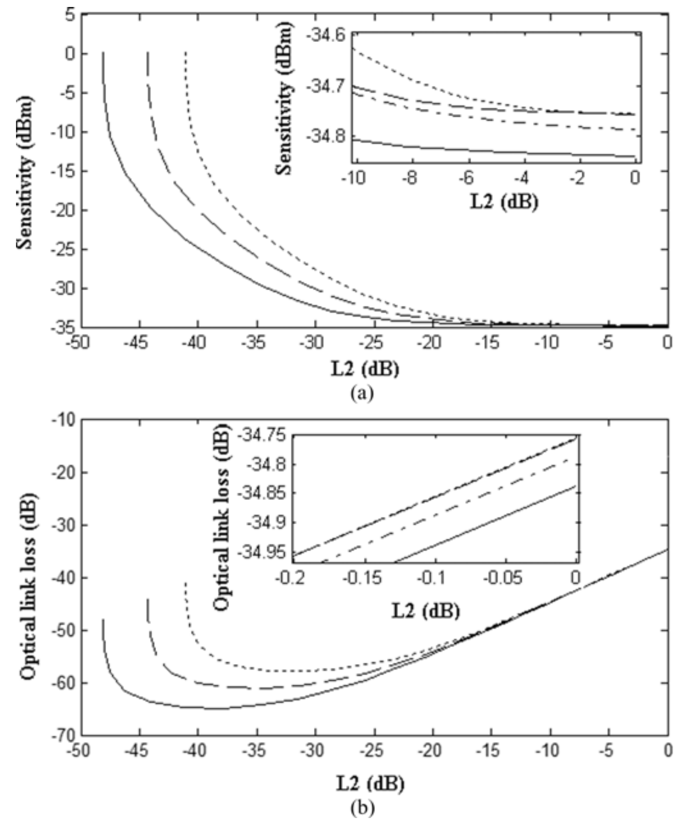

Fig. 5. Sensitivity versus L_2 (dB) [see Fig. 5(a)], and optical link loss (dB) versus L_2 (dB) [see Fig. 5(b)] for different values of τ, and $P_{\rm LO}$ (I_T = 18.5 pA/$\sqrt{}$Hz, $\text{RIN}_{\rm BN} = -149$ dB/Hz, SNRj = 13 dB). Dashed, and dashed-dotted curves are distinguishable only in enlarged pictures.

optical power must take into account a new LO-RIN reference spectral distribution [16]–[19]. Diversely, if the reference value of the LO optical power corresponds to the maximum allowable optical output power of the LO laser source, this behavior can represent a limit of the receiver which, in order to reach an optimum performance condition, can require a lower skew value, capable to reduce the LO-RIN noise variance.

Now we investigate the performances of the amplified electronically compensated link in terms of sensitivity and optical link power budget. Figs. 4–6 report the sensitivity versus L_2 (dB) (upper figures), and the allowable optical link loss (dB) versus L_2 (dB) (lower figures), obtained varying skew and LO power, in the case of a link working with $P_{\rm in} = 0$ dBm and SNR$j = 13$ dB. In these figures, we analyse the same three cases considered above. Then Fig. 4 shows results obtained with $I_T = 18.5$ pA/$\sqrt{}$Hz and $\text{RIN}_{\rm BN} = -155$ dB/Hz, Fig. 5 with $I_T = 18.5$ pA/$\sqrt{}$Hz and $\text{RIN}_{\rm BN} = -149$ dB/Hz, Fig. 6 with $I_T = 74$ pA/$\sqrt{}$Hz and $\text{RIN}_{\rm BN} = -155$ dB/Hz. In each figure, continuous curve reports results with $\tau = 0$ and $P_{\rm LO} = 16$ dBm, dotted curve with $\tau = 10$ ps and $P_{\rm LO} = 16$ dBm, dashed curve with $\tau = 10$ ps and $P_{\rm LO} = P_{\rm LOOPT}$. Dashed-dotted curve has been obtained by means of (20), assuming $\tau = 10$ ps and considering, as an optimum value of $P_{\rm LO}$, that one of the unamplified receiver: $P_{\rm LO} = P_{{\rm LOOPTW}/A}$. In all figures, we have taken into account the impact of skew on the signal by means of $k(\tau)$, equal to -0.66 dB, in correspondence of 10 ps skew.

TABLE I
UNAMPLIFIED RECEIVER SENSITIVITY ($\text{RIN}_{\rm BN}$, I_T, τ, AND $P_{\rm LO}$ AS IN FIGS. 4–6)

RIN_{BN} (dB/Hz)	I_T (pA/√Hz)	τ (ps)	P_{LO} (dBm)	P_S (dBm)
-155	18.5	0	16	-35.17
-155	18.5	10	16	-31.78
-155	18.5	10	11.47 ($P_{LOOPTW/A}$)	-32.74
-149	18.5	0	16	-35.17
-149	18.5	10	16	-27.80
-149	18.5	10	8.46 ($P_{LOOPTW/A}$)	-31.24
-155	74.0	0	16	-31.00
-155	74.0	10	16	-28.99
-155	74.0	10	17.49 ($P_{LOOPTW/A}$)	-29.18

For our analysis, we first analyse the receiver performances without amplification. Table I gives the complete picture of the unamplified receiver performances, derived with the same values of $\text{RIN}_{\rm BN}$, I_T, τ, and $P_{\rm LO}$ considered in Figs. 4–6 for the amplified receiver (signal shot noise included). First let us consider the receiver behaviour with $I_T = 18.5$ pA/$\sqrt{}$Hz. Table I shows that, in this case, the unamplified receiver works close to the shot noise limit, if the receiver is perfectly balanced (i.e., $P_S = -35.17$ dBm, with $\tau = 0$), but a significant power penalty is introduced, with 10 ps skew mismatch: for example, P_S can increase up to -31.24 dBm, if the value of $\text{RIN}_{\rm BN}$ is

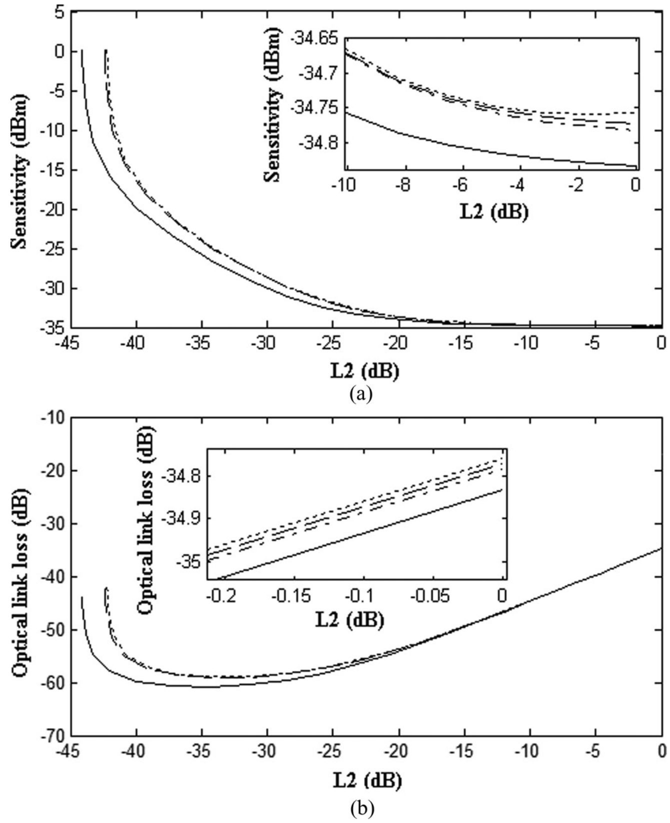

Fig. 6. Sensitivity versus L_2 (dB) [see Fig. 6(a)], and optical link loss (dB) versus L_2 (dB) [see Fig. 6(b)] for different values of τ, and $P_{\rm LO}$ (I_T = 74 pA/$\sqrt{}$Hz, $\text{RIN}_{\rm BN} = -155$ dB/Hz, SNRj = 13 dB). Dashed, and dashed-dotted curves are distinguishable only in enlarged pictures.

equal to -149 dB/Hz, although $P_{\rm LO}$ is set at the optimum value $P_{\rm LOOPTW/A}$ = 8.46 dBm. Increasing I_T up to 74.0 pA/$\sqrt{}$Hz, sensitivity strongly degrades in any case: even without introducing a receiver unbalancing, the receiver sensitivity is not better than -31.00 dBm, and increases up to -28.99 dBm, in the worst case (i.e., with $\tau = 10$ ps, and $P_{\rm LO} = 16$ dBm). As we can expect, the unamplified system reveals to be very sensitive to both the LO-RIN and the thermal noise.

Now let us consider the amplified coherent system. We firstly investigate the preamplifier configuration. In all three cases, the preamplifier configuration (obtained for $L_2 = 0$ dB, reported in the enlarged pictures) reveals to be almost independent on skew, LO-RIN, and thermal noise: according to [3], the main impact on the SNR of the amplified coherent receiver is given by the LO-ASE beat noise, which overcomes all the other noise terms, and the SNR at the preamplifier position approximates the SNR of a receiver without amplification which works close to the shot-noise limit, corresponding to the value of $P_{\rm shot} = -36.88$ dBm, given by (21). According to the theory reported above, in our picture, the sensitivity degradation produced by the receiver unbalancing is twofold, and is due to the impact of the skew on both signal and noise variances, into the SNRj expression in (4). As what regards the signal, the skew introduces, through the term $k(\tau)$, a constant power penalty of 0.66 dB in all configurations considered in the figures. As mentioned before, a higher amount of penalty—i.e., equal to 1.44 dB—could be considered in the following results, if $k_{\min}(\tau)$ in (13a) was taken into account. As what concerns the noise, the expressions of parameters defined in (14) and (15) show that the impact of the skew on the total noise variance is also twofold: enhancing skew, the signal-ASE beat noise, ASE–ASE beat noise, and LO-RIN terms increase, but the LO-ASE beat noise decreases. In fact, the CMRR_+ parameter [i.e., that one referring to the LO-ASE beat noise variance, showing the positive sign in (14c)] decreases with skew, and then the LO-ASE beat noise decreases with it as well (as reported above, we consider, for the LO_ASE beat noise, a constant noise power spectral density). This reveals an intriguing result: skew can even improve the SNR, when the LO-ASE beat noise variance is dominant (because it reduces the amount of LO-ASE beat noise in the SNR), and the SNR degradation occurs in this case only because of the impact of the skew on the signal, through term $k(\tau)$. This behavior emerges from the enlarged views reported in the figures: all of them show that, in correspondence of the preamplifier configuration, the power penalty—with respect to the results derived with $\tau = 0$—is always much less than 0.66 dB (i.e., the penalty plateau we expect to have in all the figures, due to the impact of the skew on the signal). Diversely, the power penalty in the preamplifier configuration is on the order of $\sim$ 0.05 dB, i.e., on the order of the difference in dB unit between the penalty plateau and the value of the CMRR_+ term (i.e., equal to -0.61 dB), which expresses the SNR improvement given by the LO-ASE beat noise reduction due to the skew. The slight discrepancy with this difference is due to the contributions of both the signal-ASE and ASE–ASE beat variances, which reveal to be both negligible, even in presence of a large amount of amplifier optical noise. For this reason, as it emerges from the figures, the analytical values obtained by means of the closed-form expression in (20) fit the numerical results very well.

As introduced in the previous section, this confirms that the analytical solution can be applied with an excellent degree of approximation in most of practical situations, and can result useful to calculate the performances of the optically amplified electronically compensated coherent receiver in a simple way. Another attractive result we can notice from all figures is that the performances of the preamplified receiver appear almost unaffected by LO optical power variations, if the LO optical output is high enough to be considered on the order of the power values which are commonly used in practice (i.e., $\sim$16 dBm). So, although the optimum LO power value of an amplified receiver can be very different from that of the unamplified receiver (as shown in Fig. 3(b)), in the preamplifier configuration, a satisfactory performance of the amplified receiver can be obtained with the same optimum LO power level of the unamplified receiver.

The influence of the skew on the receiver sensitivity becomes progressively different, by moving the amplifier far from the preamplifier position: the power penalty induced by the skew on the signal through the term $k(\tau)$ remains the same, but the impact of the receiver unbalancing on the total noise variance gradually changes, owing to the increasing attenuation—introduced by the fiber placed beyond the amplifier —experimented by all the ASE noise terms and, in particular, by the LO-ASE beat noise. Since the LO-ASE beat noise becomes more and more negligible, by moving the amplifier towards the booster position the skew progressively acts on the noise variance more and more through the LO-RIN, which—together with thermal noise—becomes the dominant term, in the total noise variance of the SNR. All figures show that, as the link loss beyond the amplifier increases, the amplified receiver performances gradually appear more and more similar to those ones of the unamplified receiver, which can be strongly degraded by both LO-RIN (through the unbalancing due to the skew) and thermal noise, and can heavily depend on the amount of LO optical power. Owing to the progressive reduction of the signal-ASE and ASE–ASE noise contributions, the approximated closed-form solution in (20) becomes even more and more effective, by moving the amplifier far from the receiver front end, and the analytical values reported in correspondence of dashed-dotted curves in all figures become indistinguishable from those ones of the dashed curves just after $\sim$15 dB link loss. The asymptotic behavior of the amplified receiver sensitivity with respect to L_2 (clearly visible in all figures), obtained when the amplifier approaches the booster position, is mainly due to the second term in the denominator of (20) (i.e., that one depending on the saturation power $P_{\rm sat}$), that takes into account the decrement of the amplifier gain due to the saturation, and produces an enhancement of the amplified receiver sensitivity with respect to the link loss after the amplifier. As a consequence of this functional dependence, when the amplifier is far enough from the receiver front end, the amplified receiver sensitivity results very sensitive to small variations of the link loss after the amplifier, and the sensitivity value, calculated in correspondence of a same value of $L_2 \ll 1$, can change from a curve to another one in a significant way. This behavior is well shown in Fig. 4(a): a comparison with the continuous curve (i.e., referring to $\tau = 0$) shows that, moving the amplifier far from the receiver, the sensitivity degradation induced by skew becomes more and more significant, even by setting the LO power at the optimum value. Just in this sense, a comparison of the dashed curve (i.e., with the optimum LO power) with the dotted curve (i.e., with $P_{\rm LO} = 16$ dBm) shows that, owing to the amplified receiver sensitivity asymptotic behavior, the sensitivity variations obtained in correspondence of the same value of L_2 can result relevant, when the amplifier experiments a strong gain saturation. Diversely, if the amplifier gain is quite far from saturation (i.e., in an in-line position), setting the LO optical power at the optimum value does not lead to a significant performance improvement, in comparison with the result obtained with $P_{\rm LO} = 16$ dBm, and the LO power optimization procedure cannot be considered really effective, in the case of the LO-RIN and the thermal noise considered in the figure. Curves in Fig. 4(b)—reporting the optical link losses compatible with the input power $P_{\rm in}$—are compatible with these results. The impact of the skew on the system in term of link power budget appears relevant in both the booster and in-line configuration, but is negligible in the case of the preamplifier configuration. Moreover, if the amplifier gain is near saturation, the allowable optical link loss can significantly change. On the other hand, despite of their larger vulnerability to LO-RIN and thermal noise, both booster and in-line configurations allow to get values of optical link power budget which are sensibly higher than those ones of the preamplifier. In particular, according to (25), Fig. 4(b) shows that, in each curve reported, there is an optimum in-line position of the amplifier which maximizes the optical link power budget. As predicted in the previous section, after an almost linear decrement with respect to L_2, in all figures the allowable optical link loss slowly approaches a minimum, corresponding to the optimum in-line position of the amplifier. In Fig. 4(b), the following minimum allowable link losses have been obtained: $L_{\rm TOT} = -64.88$ dB, with $L_2 = -39.15$ dB (continuous curve); $L_{\rm TOT} = -62.53$ dB, with $L_2 = -36.80$ dB (dashed and dashed-dotted curves); $L_{\rm TOT} = -61.56$ dB, with $L_2 = -35.87$ dB (dotted curve). These results are according to those ones derived by exploiting (25). According to the considerations expressed in the previous section, these values are those ones of the corresponding unamplified coherent system, whose performances are enhanced by an amount almost equal to the unsaturated value of the amplifier optical gain. As we can see from the figure, the maximum optical link power budget obtained for the optimum in-line position of the amplifier is visibly reduced by skew, but the improvement introduced by setting the LO source at the optimum LO power level is not really significant (i.e., $\sim$1 dB).

Now let us consider the results obtained when the LO-RIN noise variance increases. We can see from Fig. 5(a) that, when the receiver experiments a high LO-RIN, the amplified system is particularly sensitive to both skew and LO power in both booster and in-line configurations. In particular, a comparison between dashed and dotted curves in this figure clearly shows that reducing the LO optical power up to the optimum power value can improve the system performances in a significant way, when the amplifier is placed far from the receiver front end. In any case, the power penalty induced by the skew appears heavy, even considering the optimum LO power setting. The results derived in Fig. 5(b) are consistent with these ones: the decrement of the optical link power budget due to the skew, and the improvement introduced by setting the LO at the optimum power value are visible in the figure, when the amplifier is far from the receiver front end. In any case, even if the preamplifier position still reveals to be the most robust configuration, the optical link power budget obtained in correspondence of both booster and in-line configurations is still higher than that one of the preamplifier. In particular, the minimum allowable link losses in Fig. 5(b) are: $L_{\rm TOT} = –64.88$ dB, with $L_2 = -39.15$ dB (continuous curve); $L_{\rm TOT} = –61.08$ dB, with $L_2 = -35.36$ dB (dashed and dashed-dotted curves); $L_{\rm TOT} = –57.86$ dB, with $L_2 = -32.14$ dB (dotted curve). The improvement obtained by setting the LO at the optimum power level is now relevant, in correspondence of the optimum in-line configuration (i.e., $\sim$3.2 dB).

In Fig. 6(a), i.e., where the thermal noise is strongly enhanced, the performances of both the booster and in-line configurations are evidently influenced by skew (as we can notice by making a comparison between the continuous curve and all the other ones), but—just owing to the higher impact of thermal noise—less than in the case of Fig. 5, and the amplified system working at $P_{\rm LO} = 16$ dBm shows performances that are very close to those ones obtaining setting $P_{\rm LO} = P_{\rm LOOPT}$ (i.e., without any significant difference with the optimized case, in practice). Fig. 6(b) shows a consistent behaviour of the optical link power budget: it still reveals to be higher than that one of the preamplifier, when the amplifier is placed according to the booster and in-line configurations, and is practically independent on the LO power variation. The minima of the allowable link loss in the case of Fig. 6(b) are: $L_{\mathrm{TOT}} = -60.87$ dB, with $L_2 = -35.11$ dB (continuous curve); $L_{\mathrm{TOT}} = -59.15$ dB, with $L_2 = -33.41$ dB (dashed and dashed-dotted curves); $L_{\mathrm{TOT}} = -58.96$ dB, with $L_2 = -33.23$ dB (dotted curve). In presence of skew mismatch, the influence of the LO power appears negligible, in correspondence of the optimum in-line position (i.e., less than 0.2 dB). Finally, although we have assumed the nonlinear impairments induced by the fiber negligible or compensated by DSP, for sake of completeness we would remark that, by moving the amplifier from the optimum in-line up to the booster position, quite high values of optical power at the amplifier output have been derived: we have obtained up to $\sim$4.6 dBm, in the case of the in-line configuration, and up to $\sim$13 dBm, in the booster configuration. As we have introduced in previous section, due to the Kerr effect, these power values could strongly limit the performances of the coherent system, which could require a very sophisticated DSP compensation algorithm implemented at the receiver side.

VI. Conclusion

In summary, our investigation shows that, when the fiber impairments are fully compensated, the performances of both booster and in-line configurations are strongly dependent on the unamplified receiver features, and can require a proper adjustment of the LO optical power, to make the sensitivity compliant to requirements. In any case, even if the LO laser output is setting at the best value, the impact of the skew on the system working according to a booster or in-line configuration appears always much higher than that one obtained in correspondence of the preamplifier configuration. Diversely, in the preamplifier configuration the amplifier position makes the receiver practically independent on its intrinsic noise sources. So, just owing to its immunity to noise, the preamplifier position represents an attractive solution, from a practical point of view. On the other hand, despite of their larger vulnerability to LO-RIN and thermal noise, both booster and in-line configurations allow to get values of optical link power budget which are sensibly higher than those ones of the preamplifier. In particular, there is an optimum in-line position of the amplifier which maximizes the optical link power budget. The optimum amplifier configuration is obtained in correspondence of a distance of the amplifier from the receiver which allows the amplified coherent system to work in correspondence of an amount of the amplifier optical gain still very far from saturation, i.e., almost equal to its unsaturated value. In this condition, the maximum optical link power budget in compliance with both a required receiver performance and a fixed value of the optical power at the link input is in practice the same of that one given by the unamplified coherent receiver, increased by an amount almost equal to the unsaturated value of the amplifier optical gain. Then both booster and in-line configurations are to be preferred to that one of the preamplifier, if the DSP compensation technique is capable to overcome the linear and nonlinear effects of the fiber, and the unamplified receiver works not very far from the shot-noise limit.

Even without the support of a rigorous numerical or experimental analysis, these theoretical results appear attractive, and would be worth verifying by means of suitable experimental tests or full-field numerical simulations.

Acknowledgment

The author would like to gratefully acknowledge Prof. L. Potì of S. S. S. Anna of Pisa (Italy) for his precious hints.

References

[1] T. J. Xia, S. Gringeri, and M. Tomizawa, "High-capacity optical transport networks," *IEEE Commun. Mag.*, vol. 50, no. 11, pp. 170–178, Nov. 2012.

[2] G. Bosco, V. Curri, A. Carena, P. Poggiolini, and F. Forghieri, "On the performance of Nyquist-WDM Terabit superchannels based on PM-BPSK, PM-QPSK, PM-8QAM or PM-16QAM subcarriers," *J. Lightw. Technol.*, vol. 28, no. 4, pp. 53–61, Jan. 2011.

[3] E. Ip, A. P. T. Lau, D. J. F. Barros, and J. M. Kahn, "Coherent detection for optical fiber systems," *Opt. Exp.*, vol. 16, no. 2, pp. 753–791, 2008.

[4] G. P. Agrawal, *Fiber-Optic Communication Systems*, 2nd ed. New York, NY, USA: Wiley, 1997.

[5] A. Bononi, P. Serena, N. Rossi, E. Grellier, and F. Vacondio, "Modeling nonlinearity in coherent transmissions with dominant intrachannel-four-wave-mixing," *Opt. Exp.*, vol. 20, no. 3, pp. 7777–7791, Mar. 2012.

[6] Z. Tao, L. Dou, W. Yan, L. Li, T. Hoshida, and J. C. Rasmussen, "Multiplier-free intrachannel nonlinearity compensating algorithm operating at symbol rate," *J. Lightw. Technol.*, vol. 29, no. 17, pp. 2570–2576, Sep. 2011.

[7] C. Crognale and G. Iorio, "In-line optical amplification of a digital homodyne coherent BPSK transmission system with phase and polarization diversity," in *Proc. IEEE 8^{th} Int. Commun. Syst., Netw. Digital Signal Process.*, Poznan, Poland, Jul. 2012, pp. 8–20.

[8] B. Zhang, C. Malouin, and T. J. Schmidt, "Design of coherent receiver optical front end for unamplified applications," *Opt. Exp.*, vol. 20, no. 3, pp. 3225–3234, 2012.

[9] K. Kikuchi and S. Tsukamoto, "Evaluation of sensitivity of the digital coherent receiver," *J. Lightw. Technol.*, vol. 26, no. 13, pp. 1817–1822, 2008.

[10] Y. Han and G. Li, "Coherent optical communications using polarization multiple-input-multiple-output," *Opt. Exp.*, vol. 13, no. 19, pp. 7527–7534, 2005.

[11] K. Petermann, *Laser Diode Modulation and Noise*. Dordrecht, The Netherlands: Kluwer, 1988.

[12] N. A. Olsson, "Lightwave systems with optical amplifiers," *J. Lightw. Technol.*, vol. 7, no. 7, pp. 1071–1082, 1989.

[13] A. Fellegara and S. Bottacchi, "Analysis of power budget performances of digital transmission systems with an optical amplifier," *Electron. Lett.*, vol. 30, no. 9, pp. 717–718, 1994.

[14] A. B. Carlson, *Communication Systems—An Introduction to Signals and Noise in Electrical Communications*, 3rd ed. New York, NY, USA: McGraw Hill, 1986.

[15] G. L. Abbas, V. W. S. Chan, and T. K. Yee, "Local-oscillator excess noise suppression for homodyne and heterodyne detection," *Opt. Lett.*, vol. 8, no. 8, pp. 419–421, 1983.

[16] J.-R. Burie, G. Beuchet, M. Mimoun, P. Pagnod-Rossiaux, B. Ligat, J. C. Bertreux, J.-M. Rousselet, J. Dufour, P. Rougeolle, and F. Laruelle, "Ultra high power, ultra low RIN up to 20 GHz 1.55 μm DFB AlGaInAsP laser for analog applications," presented at the SPIE 7616, Novel In-Plane Semicond. Lasers IX, San Francisco, CA, USA 76160Y, Feb. 2010.

[17] M. C. Tatham, I. F. Lealman, C. P. Seltzer, L. D. Westbrook, and D. M. Cooper, "Resonance frequency, damping, and differential gain in 1.5μm multiple quantum-well lasers," *IEEE J. Quantum Electron.*, vol. 28, no. 2, pp. 408–414, Feb. 1992.

[18] A. Wakatsuki, Y. Kawamura, Y. Noguchi, and H. Iwamura, "Effect of conduction-band discontinuity on lasing characteristics of 1.5μm InGaAs/In(Ga)AlAs MQW-FP Lasers," *IEEE Photon. Technol. Lett.*, vol. 5, no. 4, pp. 383–386, Apr. 1993.

[19] G. E. Shtengel, G. L. Belenky, M. S. Hybertsen, R. F. Kazarinov, and D. A. Ackerman, "Advances in measurement of physical parameters of semiconductor lasers," *Int. J. High Speed Electron. Syst.*, vol. 9, no. 4, pp. 901–940, 1998.

Author biography not available at the time of publication.